

Springer Series on Fluorescence 11
Series Editor: Otto S. Wolfbeis

Gregor Jung *Editor*

Fluorescent Proteins I

From Understanding to Design

 Springer

11

Springer Series on Fluorescence

Methods and Applications

Series Editor: O.S. Wolfbeis

For further volumes:

<http://www.springer.com/series/4243>

Springer Series on Fluorescence

Series Editor: O.S. Wolfbeis

Recently Published and Forthcoming Volumes

Fluorescent Proteins II

Application of Fluorescent Protein Technology

Volume Editor: G. Jung

Vol. 12, 2012

Fluorescent Proteins I

From Understanding to Design

Volume Editor: G. Jung

Vol. 11, 2012

Advanced Fluorescence Reporters in Chemistry and Biology III

Applications in Sensing and Imaging

Volume Editor: A.P. Demchenko

Vol. 10, 2011

Advanced Fluorescence Reporters in Chemistry and Biology II

Molecular Constructions, Polymers and
Nanoparticles

Volume Editor: A.P. Demchenko

Vol. 9, 2010

Advanced Fluorescence Reporters in Chemistry and Biology I

Fundamentals and Molecular Design

Volume Editor: A.P. Demchenko

Vol. 8, 2010

Lanthanide Luminescence

Photophysical, Analytical and Biological Aspects

Volume Editors: P. Hänninen and H. Härmä

Vol. 7, 2011

Standardization and Quality Assurance in Fluorescence Measurements II

Bioanalytical and Biomedical Applications

Volume Editor: Resch-Genger, U.

Vol. 6, 2008

Standardization and Quality Assurance in Fluorescence Measurements I

Techniques

Volume Editor: U. Resch-Genger

Vol. 5, 2008

Fluorescence of Supermolecules, Polymeres, and Nanosystems

Volume Editor: M.N. Berberan-Santos

Vol. 4, 2007

Fluorescence Spectroscopy in Biology

Volume Editor: M. Hof

Vol. 3, 2004

Fluorescence Spectroscopy, Imaging and Probes

Volume Editor: R. Kraayenhof

Vol. 2, 2002

New Trends in Fluorescence Spectroscopy

Volume Editor: B. Valeur

Vol. 1, 2001

Fluorescent Proteins I

From Understanding to Design

Volume Editor:
Gregor Jung

With contributions by

C. Blum · A. Brockhinke · N. Budisa · T. Gensch · W. Gu ·
V. Helms · M.G. Hoesl · B. Hötzer · G. Jung · S. Luin ·
S.R. Meech · L. Merkel · G.U. Nienhaus · K. Nienhaus ·
R. Nifosì · S. Schwedler · V. Subramaniam ·
J.J. van Thor · V. Tozzini · S.K. Veetil · J. Wiedenmann

 Springer

Volume Editor
Dr. Gregor Jung
Professor for Biophysical Chemistry
Campus B2 2
Saarland University
66123 Saarbrücken, Germany
g.jung@mx.uni-saarland.de

ISSN 1617-1306 e-ISSN 1865-1313
ISBN 978-3-642-23371-5 e-ISBN 978-3-642-23372-2
DOI 10.1007/978-3-642-23372-2
Springer Heidelberg Dordrecht London New York

Library of Congress Control Number: 2011940868

© Springer-Verlag Berlin Heidelberg 2012

This work is subject to copyright. All rights are reserved, whether the whole or part of the material is concerned, specifically the rights of translation, reprinting, reuse of illustrations, recitation, broadcasting, reproduction on microfilm or in any other way, and storage in data banks. Duplication of this publication or parts thereof is permitted only under the provisions of the German Copyright Law of September 9, 1965, in its current version, and permission for use must always be obtained from Springer. Violations are liable to prosecution under the German Copyright Law.

The use of general descriptive names, registered names, trademarks, etc. in this publication does not imply, even in the absence of a specific statement, that such names are exempt from the relevant protective laws and regulations and therefore free for general use.

Printed on acid-free paper

Springer is part of Springer Science+Business Media (www.springer.com)

Series Editor

Prof. Dr. Otto S. Wolfbeis

Institute of Analytical Chemistry

Chemo- and Biosensors

University of Regensburg

93040 Regensburg

Germany

otto.wolfbeis@chemie.uni-regensburg.de

Aims and Scope

Fluorescence spectroscopy, fluorescence imaging and fluorescent probes are indispensable tools in numerous fields of modern medicine and science, including molecular biology, biophysics, biochemistry, clinical diagnosis and analytical and environmental chemistry. Applications stretch from spectroscopy and sensor technology to microscopy and imaging, to single molecule detection, to the development of novel fluorescent probes, and to proteomics and genomics. The *Springer Series on Fluorescence* aims at publishing state-of-the-art articles that can serve as invaluable tools for both practitioners and researchers being active in this highly interdisciplinary field. The carefully edited collection of papers in each volume will give continuous inspiration for new research and will point to exciting new trends.

Preface

A plethora of reviews, popular science books, and scientific textbooks have been written on the significance of fluorescent proteins in the life sciences. More than 30,000 references can be found in bibliographic databases which refer to at least one among the members of this protein family (see Fig. 1). Most of these narrate on how fluorescent proteins may be used to label gene products, how they may be visualized in cellular compartments by fluorescence microscopy, or how they may be expressed in individual cells, thus provoking novel findings in ontogenesis. In most of the experiments described, fluorescent proteins are being exploited as miniaturized light bulbs, the length scale is that of microns, and the time scale is that of seconds or longer. There is no doubt that fluorescent protein technology has revolutionized life sciences in that proteins have become universal and standard tools in molecular biology laboratories.

A minor fraction of roughly 5% of all publications deals with the *nanoscopic* properties of fluorescent proteins (FPs) acting as light bulbs. Early achievements include the crystallographic analysis of their molecular structure [1, 2], the discovery of excited-state proton transfer in the naturally occurring FP [3, 4], and the erratic light emission of individual members of FPs [5, 6]. Especially the last experiments, along with low temperature studies [7, 8], have revealed that FPs exhibit a tremendous heterogeneity in terms of structure and dynamics.

It is therefore not astonishing that FPs have had a large impact on other areas of biophysical research, e.g., in studies on protein folding [9–11]. However, the irregular emission of light by FPs also has impacted experiments in the life sciences: most operators of fluorescent protein technology, whom I was talking to, were concerned about weird experimental features like rapid initial fading in time-lapse microscopy, sometimes with sudden fluorescence recovery, or changing FRET-ratios upon continuous illumination. Such annoying findings can be traced back to the wealth of light-driven processes in the proteins, and I am quite sure that more surprises of that kind have been experienced by others. It should be emphasized here that such “strange” photodynamics have initiated seminal studies on protein diffusion and high-resolution microscopy [12–14].

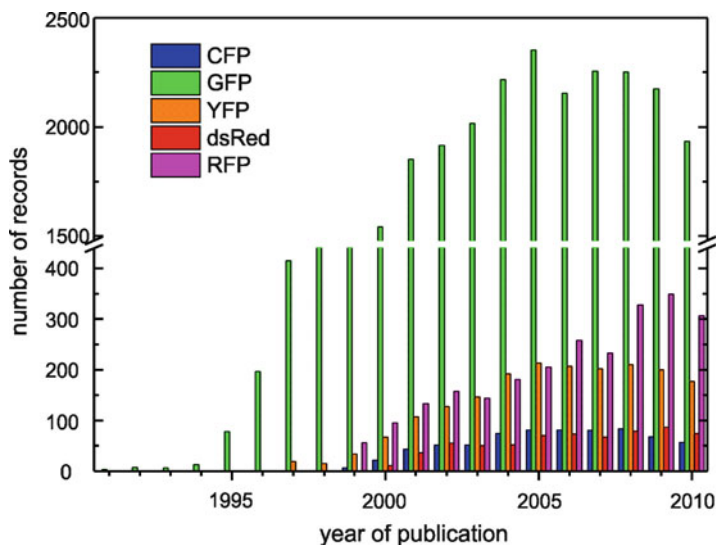


Fig. 1 Number of references related to fluorescent proteins (database: web-of-science). The number of articles dealing with Green Fluorescent Protein has reached saturation now at a level of typically 2,000 articles per year for almost a decade. Those on the Red Fluorescent Proteins are still increasing

Volumes 11 and 12 of the *Springer Series on Fluorescence* deal with various aspects of fluorescent proteins. The first volume (*Fluorescent Proteins I*) is devoted to the molecular, i.e., mainly optical, properties of fluorescent proteins. In the first part, the primary processes leading to fluorescence are discussed: excitation, relaxation, and other processes in the excited state and in emission. Fluorescence proteins are treated as “ordinary” fluorophores, and one article is highlighting our opportunities to circumvent the synthetic limitations given by nature. The second part focuses on the mechanisms that make the difference to conventional fluorophores: isomerization, protonation, as well as reversible and irreversible photochemical reactions. The knowledge on how these processes are affected by the surrounding of the FP allows for tailoring it with respect to spectacular applications, applications that are not conceivable with “ordinary” fluorophores.

In the second volume (*Fluorescent Proteins II*), the key aspect is on applications. Its first part is giving an overview on how many unconventional photophysical properties latently exist in naturally occurring and how double-resonance experiments enable the information to be extracted from microscopy data in an unprecedented way. More on high-resolution microscopy will be found in forthcoming volumes of this series. Quantitation, a central objective of analysis, is the comprehensive caption of the articles in the next part. We may state, justifiably, that researchers have reliable tools at hand to quantify some of the most abundant ions after more than a decade of development. Other physiological parameters of

overwhelming importance like the transmembrane potential still need to experience this development. The last part reports on three examples of utmost biological relevance and how ultrasensitivity in bioanalysis, i.e., single-molecule technology, is merged with FP technology. This combination has resulted in an understanding of processes on a molecular level and in detection limits that were not even thought of some 15 years ago.

A preface is also always the occasion to deeply acknowledge the support by others. First of all, I have to thank my family who tolerated my commitment to this experience. I also would like to express my thanks to my coworkers, to my colleagues, and to the representatives of Saarland University for their understanding. In times of growing competitiveness in many academic areas, it is not self-evident to dedicate a substantial amount of time to such a book project. For the same reason, I especially appreciate the immense work of all authors of these two volumes who are all passionate, but busy scientists and who (more or less) voluntarily spared no pains to complete their manuscripts in a wonderful and highly professional way. By now, it also may be appropriate to apologize for my e-mail bombardments!

Saarbrücken, Germany

Gregor Jung

References

1. Ormö M et al (1996) *Science* 273:1392–1395
2. Yang F et al (1996) *Nat Biotechnol* 14:1246–1251
3. Chattoraj M et al (1996) *Proc Natl Acad Sci USA* 93:8362–8267
4. Lossau H et al (1996) *Chem Phys* 213:1–16
5. Dickson R et al (1997) *Nature* 388:355–358
6. Pierce D et al (1997) *Nature* 388:338
7. Creemers T et al (1999) *Nat Struct Biol* 6:557–560
8. Seebacher C et al (1999) *J Phys Chem B* 103:7728–7732
9. Craggs T (2009) *Chem Soc Rev* 38:2865–2875
10. Hsu S et al (2009) *Chem Soc Rev* 38:2951–2965
11. Mickler M et al (2007) *Proc Natl Acad Sci USA* 104:20268–20273
12. Yokoe E, Meyer T (1996) *Nat Biotech* 14:1252–1256
13. Patterson G, Lippincott-Schwartz J (2002) *Science* 297:1873–1877
14. Betzig E et al (2006) *Science* 313:1642–1645

Contents

Part I Basics and Manipulation of Light-Matter Interaction in Fluorescent Proteins

One-Photon and Two-Photon Excitation of Fluorescent Proteins	3
Riccardo Nifosì and Valentina Tozzini	
Primary Photophysical Processes in Chromoproteins	41
Stephen R. Meech	
Fluorescence Lifetime of Fluorescent Proteins	69
Gregor Jung, Andreas Brockhinke, Thomas Gensch, Benjamin Hötzer, Stefanie Schwedler, and Seena Koyadan Veettil	
Synthetic Biology of Autofluorescent Proteins	99
Michael Georg Hoesl, Lars Merkel, and Nediljko Budisa	

Part II Switching on the Molecular Level

Vibrational Spectroscopy of Fluorescent Proteins: A Tool to Investigate the Structure of the Chromophore and Its Environment	133
Valentina Tozzini and Stefano Luin	
Proton Travel in Green Fluorescent Protein	171
Volkhard Helms and Wei Gu	
Photoconversion of the Green Fluorescent Protein and Related Proteins	183
Jasper J. van Thor	

Spectral Versatility of Fluorescent Proteins Observed on the Single Molecule Level	217
Christian Blum and Vinod Subramaniam	
Structure–Function Relationships in Fluorescent Marker Proteins of the Green Fluorescent Protein Family	241
G. Ulrich Nienhaus, Karin Nienhaus, and Jörg Wiedenmann	
Index	265

Part I
Basics and Manipulation of Light-Matter
Interaction in Fluorescent Proteins

One-Photon and Two-Photon Excitation of Fluorescent Proteins

R. Nifosì and V. Tozzini

Abstract Fluorescent proteins (FPs) offer a wide palette of colors for imaging applications. One purpose of this chapter is to review the variety of FP spectral properties, with a focus on their structural basis. Fluorescence in FPs originates from the autocatalytically formed chromophore. Several studies exist on synthetic chromophore analogs in gas phase and in solution. Together with the X-ray structures of many FPs, these studies help to understand how excitation and emission energies are tuned by chromophore structure, protonation state, and interactions with the surrounding environment, either solvent molecules or amino acids residues. The increasing use of FPs in two-photon microscopy also prompted detailed investigations of their two-photon excitation properties. The comparison with one-photon excitation reveals nontrivial features, which are relevant both for their implications in understanding multiphoton properties of fluorophores and for application purposes.

Keywords Fluorescent proteins · Chromophore structures · Computational studies · Isolated chromophores · Multiphoton spectroscopy · Structure-property relationship · Spectral tuning

Contents

1	Introduction	4
2	<i>av</i> GFP: Structure and Optical Properties	4
2.1	Structure and Chromophore Formation	5
2.2	Absorption, Excitation, and Emission	6
3	Chromophores of FPs	8
4	Isolated Chromophores	11
4.1	Model Chromophores in Gas Phase and in Solution	15
4.2	Chromophores of FPs: Computational Studies	16
5	FPs Spectra: Spectral Tuning by the Protein Environment	20

R. Nifosì (✉) and V. Tozzini
NEST CNR-NANO, Piazza San Silvestro 12, 56126 Pisa, Italy
e-mail: r.nifosi@sns.it

5.1	Proteins with GFP Chromophore	21
5.2	Proteins with RFP Chromophore	27
6	Two-Photon Excitation	29
7	Outlook	34
	References	34

1 Introduction

By the term fluorescent proteins (FPs), it is customary to indicate all fluorescent homologues of the original *Aequorea victoria* green fluorescent protein (GFP or *avGFP*). An accessory protein of the bioluminescence system of jellyfish *A. victoria*, *avGFP* was discovered as early as the 1960s [1]. Thirty years later, with the cloning of the gene [2] and the demonstration that its expression in other organisms generates fluorescence [3, 4], interest in GFP began to rise dramatically. Since then, it has triggered a revolution in bioimaging by fluorescence microscopy [5]. Soon, many other fluorescent and nonfluorescent GFP homologues were discovered in a variety of sea organisms, such as reef corals and sea anemones [6]. Further discoveries and mutagenesis engineering have produced a profusion of FPs with optical properties spanning most of the visible spectrum and beyond.

Fluorescence in FPs stems from the presence of a chromophore moiety, formed within the conserved β -barrel fold via a mechanism entailing autocatalytic backbone cyclization at an internal tripeptide sequence. Distinct postcyclization processing leads to different chromophore structures. The multiplicity of optical properties of FPs is surely one of the factors that contribute to their usefulness. It primarily arises from the different chemical structures of the chromophore. A finer tuning originates from the noncovalent interactions of the chromophores with the surrounding molecular matrix.

This chapter focuses on the mechanisms behind this spectral tuning, covering both experimental and theoretical/computational work. The reader is first presented with the more familiar case of *avGFP*. The chromophore structures of other FPs are described in Sect. 3. The following section surveys various studies on synthetic analogs of chromophores of FPs in gas phase and in solution. Section 5 provides a detailed description of spectral modifications due to interactions between chromophore and surrounding protein matrix. Finally, the last section covers two-photon properties of FPs. Several other reviews on FP optical properties are available, some treating more exhaustively the variety of GFP-like fluoro and chromoproteins, and other more focused on application purposes. For recent surveys, see [7–9].

2 *avGFP*: Structure and Optical Properties

The first to be cloned [2] and functionally expressed in other organisms [3, 4], *avGFP* has actually been replaced in most applications by its mutants and homologues. Nonetheless, being one of the best characterized in terms of optical and photophysical properties, it is a suitable starting point to introduce the concepts recurring in this chapter.

2.1 Structure and Chromophore Formation

The 238 amino acid (27 kDa) long sequence of *av*GFP folds in a compact cylindrical form called β -barrel, its lateral wall being an 11-stranded β -sheet (Fig. 1) [10, 11]. Several X-ray structural studies support the notion that also all other FPs share the β -barrel fold. They can differ in quaternary structure, though most natural FPs are tightly bound tetramers and some are dimers, a feature that initially hampered their applications. However, mutagenesis studies were able in most cases to produce viable monomeric variants of the parent proteins.

The β -barrel is capped on both ends by short α -helical sections and traversed by an α -helix segment. This segment contains the chromophore, a 4-(*p*-hydroxybenzylidene) imidazolinone, originating from the posttranslational cyclization of three consecutive amino acids at position 65–67, such as Ser, Tyr, and Gly. As demonstrated by the fact that expression of *av*GFP gene in other organisms leads to fluorescence, the posttranslational synthesis of the chromophore does not require any jellyfish-specific enzyme [3, 4]. It requires, however, exogenous oxygen, in the absence of which GFP does not develop fluorescence [4, 12].

Chromophore formation (Fig. 2) proceeds within the native fold (i.e., no chromophore is formed under denaturing conditions). It first entails backbone cyclization at the Ser65-Tyr66-Gly67 tripeptide through nucleophilic attack of the amide group of Gly67 onto the carbonyl group of Ser65, promoted by Arg96, a conserved residue in all natural FPs (see [13] and references therein). Molecular oxygen is required for the subsequent oxidation reaction. One water molecule is also abstracted from the structure, with most experimental studies supporting the cyclization–oxidation–dehydration sequence of events [13, 14].

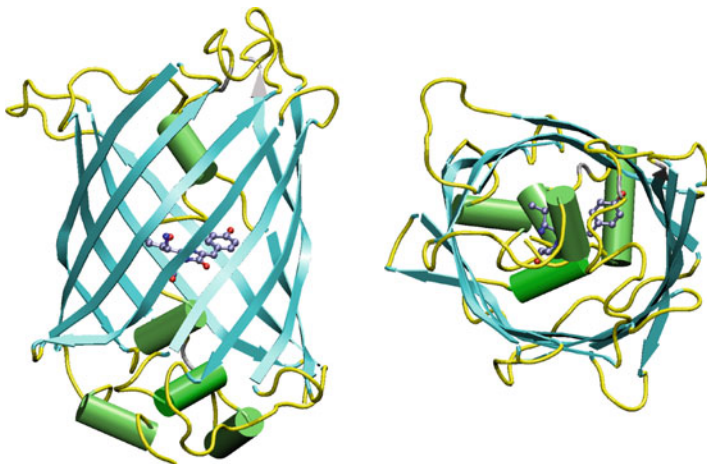


Fig. 1 Tertiary structure of *av*GFP. The usual cartoon representation is used, where α -helices are cylinders and β -sheets arrows. The chromophore is shown in a ball-and-sticks representation with the standard coloration for atom elements (i.e., gray for carbon, blue for nitrogen, and red for oxygen)

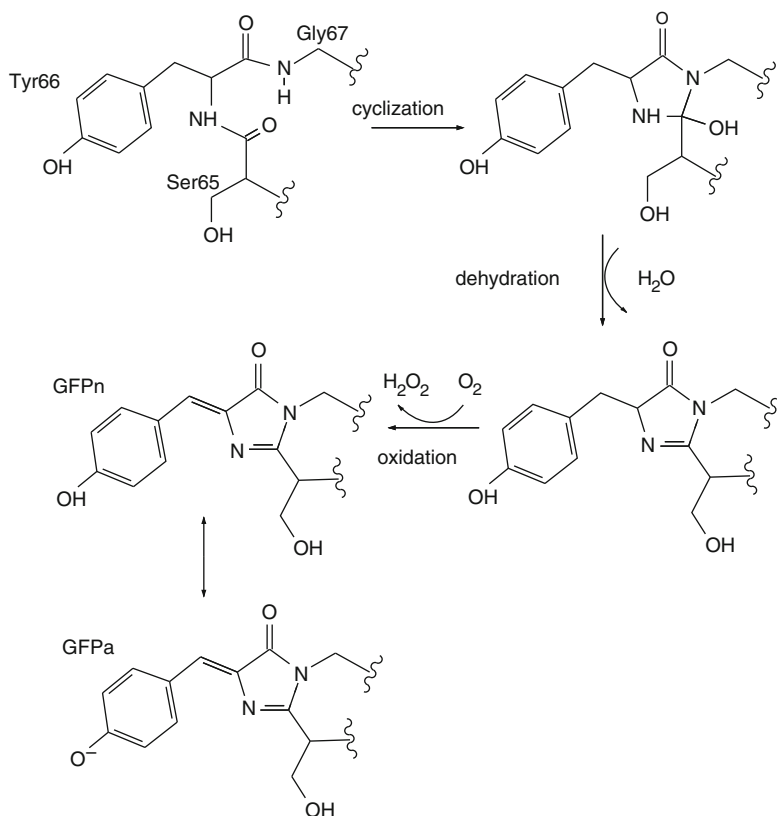


Fig. 2 Proposed mechanisms of biosynthesis of the GFP chromophore. In the last step of the reaction, the two relevant protonation states are shown

The mature chromophore consists of two rings, the phenol ring, coming from the side chain of Tyr66, and the five-member heterocyclic ring (imidazolinone), resulting from the cyclization of the backbone. The imidazolinone core is a common feature of all known FP chromophores. The alternating single and double bonds in the bridge region extend the electron delocalization from the phenolate to the carbonyl of the imidazolinone. Efficient visible-light absorption is ultimately determined by this π -conjugated system, i.e., the single–double bond alternation with connected atomic p-orbitals.

2.2 Absorption, Excitation, and Emission

The room temperature absorption, excitation, and emission spectra of *av*GFP are shown in Fig. 3. Apart from the 278-nm band, which is common to proteins containing aromatic amino acids, *av*GFP exhibits a major absorption band at

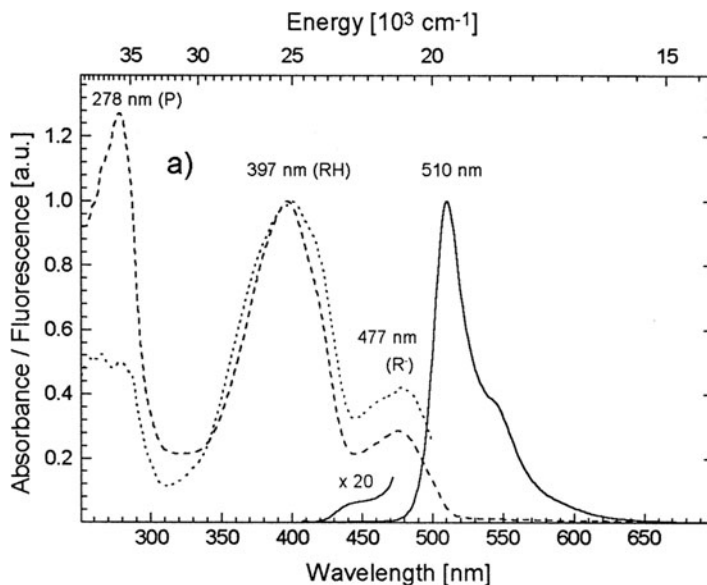


Fig. 3 Room temperature absorption (*dashed line*), fluorescence excitation (*dotted line*) and emission spectra (*solid line*) of avGFP, at room temperature and pH 8.0 (adapted from Kummer et al. [15])

397 nm and a minor band at 477 nm, due to absorption of the chromophore. Their relative height depends on proton concentration: increasing pH above 11, the minor lower-energy band increases at the expense of the higher-energy band. Vice versa, at pH below 4 the minor energy band is completely depleted [16]. The relative population in Fig. 3 is rather constant between pH 6 and 11. This behavior arises from the ground-state equilibrium between two states of the chromophore, differing in protonation of the phenolic group from Tyr66. The phenolic oxygen of the chromophore is protonated in the state absorbing at 397 nm (RH in the following) and deprotonated in that absorbing at 477 nm (state R^-). It is commonly accepted that the two other possible protonation sites in the chromophore, i.e., the nitrogen and the carbonyl oxygen of the imidazolinone, are deprotonated in both the absorbing states, thereby giving an overall neutral chromophore in state RH (GFPn in Fig. 2) and anionic in state R^- (GFPa) [17].

Excitation of state RH leads to a fluorescence spectrum peaking at 510 nm (Fig. 3), with a rather high quantum yield of 0.79. State R^- yields a similar fluorescence spectrum, slightly blueshifted and peaking at 503 nm (not shown). In both cases, fluorescence comes from emission of the singlet excited state of the anionic chromophore. Excitation of the neutral chromophore results in ultrafast (4 ps) excited state proton transfer (ESPT) and subsequent emission of the anionic form [18]. The ESPT acceptor has been identified in (deprotonated) Glu222 [18, 19].

Although the anionic chromophore is the emitting species in both states, the configuration of the surrounding residues is different and the decay time of the

excited state (few ns) is too short to allow equilibration, resulting in the observed slight shift of emission peak (510–503 nm).

3 Chromophores of FPs

Chromophore structures of FPs and their formation mechanisms are summarized in Fig. 4. The range of excitation and emission wavelengths that they give rise to in different representative FPs can be read in Table 1.

In all natural FPs discovered so far, the prechromophore tripeptide has a X_1 -Tyr₂-Gly₃ sequence, where X_1 can be almost any amino acid. Chromophore formation is inhibited upon mutation of the Gly₃ [13], suggesting that the peculiar conformational flexibility of Glycine is necessary at that location. By contrast, substitution of Tyr₂ with an aromatic amino acid (Phe, His, or Trp) preserves the fluorescence. The resulting artificial mutants contain chromophores with the phenol ring replaced by the corresponding aromatic ring, and have blueshifted excitation and fluorescence wavelengths with respect to the parent protein. Blue FPs such as EBFP [118], Azurite [22], and EBFP2 [21] all derive from Y66H *av*GFP (BFP chromophore in Fig. 4) with additional mutations to improve folding efficiency, brightness, and photostability. Y66W *av*GFP mutants (CFP in Fig. 4) such as Cerulean [23] and ECFP [11] emit cyan light.

The other determinant of chromophore structure comes from modifications around the X_1 α -carbon. With respect to the *av*GFP chromophore formation mechanism, an additional step occurs in DsRed [43] and other red fluorescent proteins (RFPs), namely the oxidation of the C–N main-chain bond of X_1 , which leaves an acylimine substituent at the corresponding position of the imidazolinone ring. The sequence of events during RFP chromophore self-processing entails first the oxidation leading to the acylimine substituent followed by dehydrogenation of the bridging carbon [14]. The acylimine substituent enlarges the extension of the π -conjugated system, and correspondingly lowers the excitation energy, resulting in red/orange fluorescence. Analogously to the case of the GFP chromophore, substituting the Tyr₂ in this chromophore with Phe or Trp (RFP Y67F and RFP Y67W in Fig. 4) results in blueshifted spectral properties, with fluorescence in the blue (mBlueberry2 [21]) and orange (mHoneydew [32]) domain, respectively.

In eqFP611 and Rtms5, the RFP chromophore is in the *trans* (or E) isomer instead of the *cis* (or Z) form normally present in other FPs [39, 44]. It adopts a coplanar conformation in eqFP611, whereas in Rtms5 it is highly non-coplanar. This feature is linked with the very different quantum yields of the two proteins, presumably because noncoplanar conformations favor non-radiative de-excitation pathways [44].

Further reactions can take place around the acylimine moiety, such as side chain cyclization by nucleophilic addition of the Thr (in mOrange), Cys (mKO), or Lys (zFP538) side chain, the latter followed by backbone cleavage [45–47]. Backbone

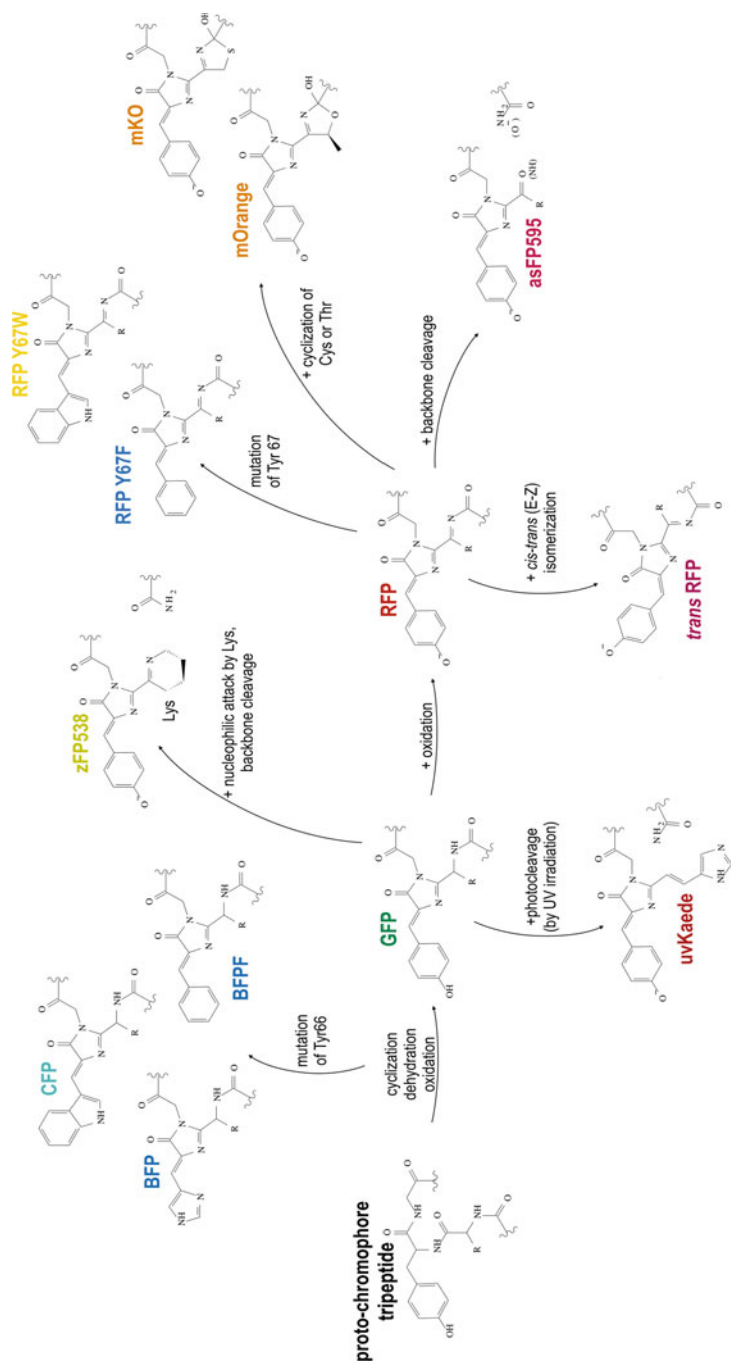


Fig. 4 Chromophore structures and reactions leading to mature chromophores in fluorescent proteins

Table 1 Optical properties of representative fluorescent proteins

Name ^a	Original protein	Chromophore ^b	Exc/Abs peak (nm)	Em peak (nm)	Ext. coeff (10 ³ M ⁻¹ cm ⁻¹)	QY ^c	References
GFP Y66F	<i>av</i> GFP	BFPF	360	442	-	(low)	[11]
EBFP	<i>av</i> GFP	BFP	377	446	30	0.15	[20]
EBFP2	<i>av</i> GFP	BFP	383	448	32	0.56	[21]
Azurite	<i>av</i> GFP	BFP	384	450	26.2	0.55	[22]
mKalama1	<i>av</i> GFP	GFPn	385	456	36	0.45	[21]
mBlueberry2	DsRed	RFP Y67F	402	467	51	0.48	[21]
Cerulean	<i>av</i> GFP	CFP	433	475	43	0.62	[23]
ECFP	<i>av</i> GFP	CFP	434	476	32.5	0.4	[115]
mTFP1-Y67W	amFP486	CFP	424/440 ^d	461/482 ^d	13	0.02	[24]
cFP484 (tetr)	-	GFPa	456	484	35.3	0.48	[6]
amFP486 (tetr)	-	GFPa	458	486	40	0.24	[6]
mTFP1	amFP486	GFPa	462	492	64	0.85	[24]
EGFP	<i>av</i> GFP	GFPa	484	507	53	0.6	[20]
<i>av</i> GFP R state ^c	-	GFPa	477	508	9.5	0.72	[116]
<i>av</i> GFP RHstate	-	GFPn	397	510 (ESPT) ^f	25	0.78	[116]
T-Sapphire	<i>av</i> GFP	GFPn	399	511 (ESPT)	44	0.60	[25]
Dronpa	22G	GFPa	503	518	95	0.85	[26]
EYFP	<i>av</i> GFP	GFPa	514	527	84	0.61	[27]
Venus	<i>av</i> GFP	GFPa	515	528	92.2	0.57	[28]
YPet	<i>av</i> GFP	GFPa	517	530	104	0.77	[29]
PhiYFP (dim)	-	GFPa	525	537	115	0.60	[30]
zFP538 (dim)	-	zFP538	528	538	-	0.42	[6]
mKO	KO	mKO	548	561	51.6	0.60	[31]
mHoneydew	DsRed	RFP Y67W	487/504 ^d	537/562 ^d	17	0.12	[32]
mOrange	DsRed	mOrange	548	562	71	0.69	[32]
Dendra <i>pa</i> ^g	DendFP	uvKaede	557	575	20	0.72	[33]
EosFP <i>pa</i> (tetr)	-	uvKaede	571	581	41	0.55	[34]
Kaede <i>pa</i> (tetr)	-	uvKaede	572	582	60.4	0.33	[35]
DsRed (tetr)	-	RFP	558	583	57	0.79	[6]
asFP595 <i>pa</i> (tetr)	-	asFP595	568	595	56.2	<10 ⁻³	[36]
mStrawberry	DsRed	RFP	574	596	90	0.29	[32]
KFP1 <i>pa</i> (tetr)	AsFP595	asFP595	580	600	59	0.07	[117]
mRFP1	DsRed	RFP	584	607	44	0.25	[37]
mCherry	DsRed	RFP	587	610	72	0.22	[32]
eqFP611 (tetr)	-	<i>trans</i> RFP	559	611	78	0.45	[38]
Rtms5 (tetr)	-	<i>trans</i> RFP	592	620	80	<10 ⁻³	[39]
mPlum	DsRed	RFP	590	649	41	0.10	[40]
mNeptune	eqFP578	RFP	600	650	67	0.20	[41]
cjBlue	-	RFP	610	-	66.7	-	[42]

^aThe oligomerization state, i.e., dimer (dim) or tetramer (tetr), is reported for nonmonomeric proteins

^bChromophore name refers to Fig. 4

^cQY = Quantum yield

^dTwo excitation/fluorescent peaks are present

^eRH state and R⁻ state for *av*GFP refer to the two bands assigned to neutral (GFPn) and anionic (GFPa) protonation state of the chromophore

^fESPT in the fourth column indicates that emission from the anionic species takes place after excited state proton transfer

^g*pa* = after photoactivation

cleavage also occurs in asFP595 [48, 49].¹ AsFP595 is normally nonfluorescent and contains a *trans* (E) chromophore. Its fluorescent form is accessed either temporarily or permanently by photoactivation (hence the alternative name kindling fluorescent protein, or KFP), and contains a *cis* (Z) chromophore.

A different mechanism of redshifting occurs in Kaede and related proteins (KikGR, EosFP, Dendra), where UV excitation photoconverts the originally green-emitting proteins (with a GFP-like chromophore) into RFPs by cleaving the backbone between main-chain N and C α of the Histidine at X₁. The cleavage is followed by double-bond formation between C α and C β giving rise to the uvKaede chromophore structure [34, 35].

As in avGFP, chromophores with the phenol group exist as either neutral (protonated phenol) or anionic (deprotonated phenol). The absorption of the neutral form is always significantly blueshifted with respect to the anionic form. Changing the buffer pH generally results in a fluorescence titration curve that reveals the changing equilibrium between these two forms. Several FPs at physiological pH contain only the anionic chromophore. avGFP and some of its mutants are exceptions to this general behavior, because they can present both states, existing in a persistent equilibrium over a broad pH range.

It is worth mentioning that according to some computational investigations, in some proteins, such as asFP595, the zwitterionic form (with the imidazolinone nitrogen protonated) might be the emitting one [51]. In addition, the zwitterionic and other protonation state such as the cationic form (protonated phenol and imidazolinone) may be involved in FP photophysics [52]. The cation, however, exists at too acidic conditions (pH < 2) from studies of chromophore analogs in solution [17, 53], in which the protein is denatured. Hence, it is not considered relevant to FPs optical response at physiological conditions.

4 Isolated Chromophores

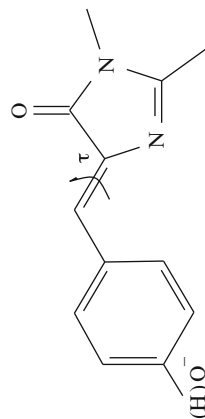
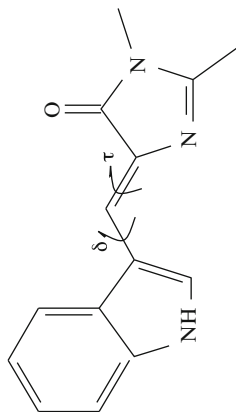
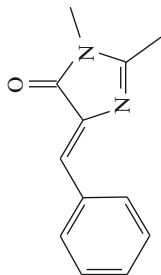
Synthetic analogs of chromophores of FPs were the starting point for a variety of experimental and computational studies aiming to examine all the factors influencing optical properties of FPs. Isolated chromophore models in solution are poorly, if at all, fluorescent at room temperature. However, they become fluorescent when the temperature is lowered to 77 K [54]. Presumably the conformational freedom at higher temperature enables non-radiative pathways of de-excitation.

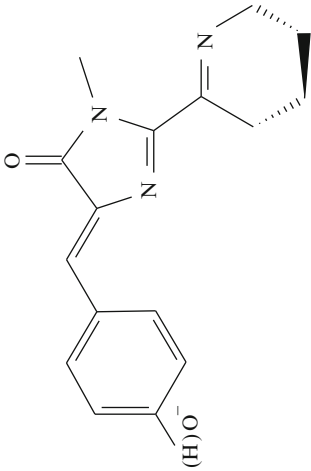
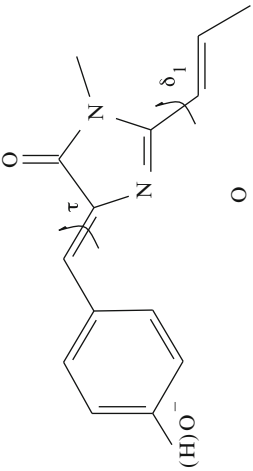
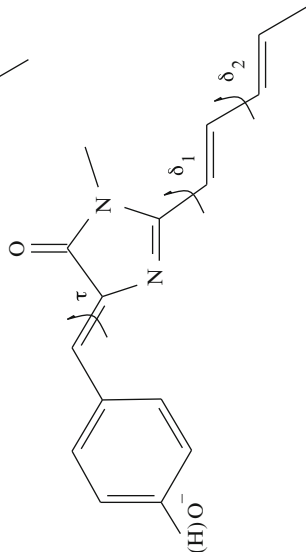
The established experimental model for the GFP chromophore is a *p*-hydroxybenzylidene-2,3-dimethylimidazolone or *p*-HBDI (Table 2). Such a model encompasses the relevant π -conjugated system. It lacks, however, the side chain of X₁ (the first residue of the tripeptide). That *p*-HBDI is a fairly accurate model for the

¹AsFP595 chromophore structure has been subject to debate, regarding the possible presence of an imino (NH) group in place of the keto group at position 2 of the imidazolinone (see discussion in [50]).

Table 2 Synthetic model chromophores and their absorption peaks in gas phase and in solution

Name	Chromophore model		Gas-phase abs peak in nm		Solution abs peak in nm (extinction coefficient $\text{mM}^{-1} \text{cm}^{-1}$, when available)		
	Anionic	Cationic	Anionic	Cationic	Neutral	Anionic	Cationic
BFPP^a	-	-	-	-	348 water 348 metOH 353 CH ₃ CN 355 dioxane 357 toluene	-	-
CFP^{a,b}	-	-	-	-	405 water 402 metOH 388 CH ₃ CN 390 dioxane 389 toluene	-	-
p-HBDJ^c (GFP model chrom.) <i>pK_a</i> = 8.1 ^d	479	406	425 water 428 metOH 433 dioxane 462 DMF 471 DMSO 482 pyridine	372 water 367 metOH 362 dioxane 368 DMF 370 DMSO 372 pyridine	387 water 398 metOH 397 dioxane 378 DMF 383 DMSO	-	-



<p>Model chrom. of zFP538^c</p> 	-	-	417 water	530 water	-
<p><i>p</i>-HBMPJ^f (RFP1, RFP model chrom.)</p> 	521	441	401 water 397 CH ₃ CN	460 water 492 CH ₃ CN	416 water 419 CH ₃ CN
<p><i>p</i>-HBMPDJ^g (RFP2, RFP model chrom.)</p> 	549	448	421 water 419 CH ₃ CN	482 water 515 CH ₃ CN	443 water 448 CH ₃ CN

(continued)

Table 2 (continued)

Name	Chromophore model	Gas-phase abs peak in nm		Solution abs peak in nm (extinction coefficient mM ⁻¹ cm ⁻¹ , when available)		
		Anionic	Cationic	Neutral	Anionic	Cationic
Model of uvKaede chrom. (red form, after photocleavage) ^b <i>pKa</i> = 7.7		-	-	430 (41) water 443 (40) etOH 444 (41) prOH 446 (40) DMF 448 (37) DMSO	490 (53) water 502 (79) etOH 514 (80) prOH 557 (77) DMF 565 (80) DMSO	-
AHBM1 (Model of asFP595 chrom.) ^c <i>pKa</i> = 7.1		-	-	418 (35) water 425 (40) etOH 428 (39) 2-prOH 422 (38) DMF	520 (47) water 542 (72) etOH 552 (73) 2-prOH 572 (87) DMF	-

^aSolution values from Vollani et al. [55]^bDihedrals describing different conformational isomers are indicated^cGas-phase values from Nielsen et al. [56]; solution values from Dong et al. [57]^dThe *pKa* for the anionic-neutral transition is indicated^eSolution values from Yampolsky et al. [58]^f*p*-4-Hydroxybenzylidene-1-methyl-2-propenyl-imidazolinone. Gas-phase values from Boy et al. [59]; solution values from He et al. [84]^g*p*-4-Hydroxybenzylidene-1-methyl-2-penta-1,3-dien-1-yl-imidazolinone. Gas-phase values from [59]; solution values from He et al. [84]^hSolution values from Yampolsky et al. [60]ⁱ(2-Acetyl-4-(*p*-hydroxybenzylidene)-1-methyl-5-imidazolone. Solution values from Yampolsky et al. [50]

isolated chromophore is implied by the similarity between its (solution) absorption spectrum and that of the denatured GFP [61], where the chromophore is presumed to be completely exposed to the solvent. Varying the solution pH, anionic, neutral, and cationic forms of *p*-HBDI are obtained, with $pK_a \sim 8$ for the anionic to neutral reaction and $pK_a \sim 2$ for the neutral to cationic reaction [17, 57].

Analogous blue fluorescent protein (BFP, with the Y66H mutation), BFPF (BFP, with Y66F), and cyan fluorescent protein (CFP, with Y66W) chromophore models were synthesized [55]. Attempts to synthesize models for the RFP chromophore revealed that the compound with the acylimine group is not stable in solution, due to the susceptibility of acylimines to nucleophilic attack. Hence, currently available models for the RFP chromophore, namely *p*-HBMPI and *p*-HBMPDI, contain an olefinic substituent in place of the acylimine group [59].

4.1 Model Chromophores in Gas Phase and in Solution

4.1.1 Gas Phase

Gas-phase absorption spectra of anionic *p*-HBDI ($p\text{-HBDI}^-$) were measured in photo destruction spectroscopy experiments [56]. Charged molecules trapped in an electrostatic ion storage ring are irradiated with laser light, and the yield of neutral fragments, produced by photochemical processes upon photon absorption, is measured as a function of the excitation wavelength. Using this technique, Andersen and coworkers reported an absorption peak of 479 nm for $p\text{-HBDI}^-$ [56]. Such a value is very close to the absorption of the R^- state (anionic chromophore) in *av*GFP. The authors conclude that, in this protein, the arrangement of the side chains and water molecules around the chromophore produces a situation more similar to the gas phase than to solution, where the absorption is blueshifted (see below).

A new set of experiments by Forbes and Jockusch [62] on $p\text{-HBDI}^-$ were able to expand the spectral window of detection, and to distinguish two photo degradation channels contributing to the total spectrum. One, closely matching the spectrum previously measured by Andersen and coworkers, corresponds to the loss of one of the two methyl groups. The other appears at higher energies (peak at 410 nm) and is attributed to electron detachment. No fluorescence is detected upon excitation [62].

Similar experiments on the anionic *p*-HBMPI and *p*-HBMPDI (RFP model chromophores) yielded absorption peaks at 521 and 549 nm, respectively [59, 63]. The latter value is closer to the absorption maximum of DsRed, at 558 nm [6]. The spectra also display a well-resolved progression of vibronic peaks with vibrational spacing of 10 nm (382 cm^{-1}) and 16 nm (518 cm^{-1}) for *p*-HBMPI and *p*-HBMPDI, respectively. The width of the spectra is hence due to both vibronic and inhomogeneous broadening effects.

Cationic forms *p*-HBDI [64], *p*-HBMPI, and *p*-HBMPDI [63] were also investigated, resulting in peaks at 406, 441, and 448 nm.

The electrostatic storage clearly requires charged molecules. Thereby, the neutral protonation state, despite relevant to GFP (and other FPs) optical properties, was

initially neglected. Recently, a model for the neutral chromophore was devised by adding a methyleneammonium cation to *p*-HBDI, charging the molecule at a site sufficiently detached from the conjugated system. The spectrum of this model compound peaks at 399 nm [65], close to absorption of the neutral band of *av*GFP. How well this model describes the neutral chromophore was discussed in [66].

4.1.2 Solution

With respect to gas-phase experiments, absorption of *p*-HBDI⁻ in water is blue-shifted and exhibits a rather broad band peaking at 425 nm [17, 57] (see Table 2). In nonpolar solvents, the absorption maximum is at 440 ± 5 nm. Increased solvent polarity yields redshifted values. The longest wavelength peak, 482 nm, was recorded in pyridine. The wavelength shift in going from water to pyridine is rather sizable (57 nm) and corresponds to an energy shift of $2,755 \text{ cm}^{-1}$ (0.34 eV). Using the multivariant Kamel–Taft fit on the data in these various solvents, one can extrapolate a value of 437 nm (2.84 eV) for the gas-phase, i.e., a solute with zero acidic, basic, and polar parameters [57].

The significant solvatochromic shift of the anionic state points to a marked sensitivity to the surrounding environment. Such sensitivity emerges also when the chromophore is embedded in the protein matrix: in different FPs, the absorption corresponding to the anionic chromophore shows a similar, if not larger, range of variation (see Sect. 5.1). Absorption of neutral and cationic *p*-HBDI peaks at 368 and 393 nm respectively, and displays a much narrower solvatochromism (variation of ~ 20 nm, around $1,000 \text{ cm}^{-1}$).

Besides the main band, reported in Table 2, the absorption spectra of both neutral and anionic *p*-HBDI reveal features at shorter wavelength (around 300 and 250 nm for *p*-HBDI and at 320 nm for *p*-HBDI) [55, 57]. Similar blueshifted bands are also measured in AHBMI (model chromophore of asFP and KFP) [50] and in model chromophores of BFPF, BFP, [55], and Kaede [60]. Features around 330 nm are also detectable in red FPs [67]. In *av*GFP, by contrast, these excitations merge with the absorption of other aromatic residues in the protein. Excitation to these states is characterized in some cases by strong two-photon cross-section (see Sect. 6).

As stated above, solvated model chromophores are generally poorly fluorescent at room temperature [54, 68]. For instance, the chromophore fluorescence quantum yield in DMF (dimethylformamide) is 0.00005 [60]. More appreciable fluorescence is instead displayed by AHBMI and by uvKaede chromophore models in DMF solution, with fluorescence quantum yields of 0.0021 and 0.005, respectively [50, 60].

4.2 Chromophores of FPs: Computational Studies

Quite a number of theoretical/computational studies were dedicated to the optical spectra of model chromophores of FPs in the gas phase [66, 69–76]. Attempts to